Deep Learning Based Rectum Segmentation on Low-field Prostate MRI to Assist Image-guided Biopsy

Huong Pham[1], Dang Bich Thuy Le[2], Meredith Sadinski[2], Ram Narayanan[2],

Aleksandar Nacev[2], Bin Zheng[1]

[1]School of Electrical and Computer Engineering, University of Oklahoma, Norman, OK 73019, USA

[2]Promaxo, Oakland, CA 94607, USA

ABSTRACT

Efficient and accurate segmentation of the rectum in images acquired with a low-field (58-74mT), prostate Magnetic Resonance Imaging (MRI) scanner may be advantageous for MRI-guided prostate biopsy and focal treatment guidance. However, automated rectum segmentation on low-field MRI images is challenging due to spatial resolution and signal-to-noise ratio (SNR) constraints. This study aims to develop a deep learning model to automatically segment the rectum in a low-field MRI prostate image. 132, 3D images from 10 patients were assembled. A 3D, U-Net model with the input matrix size 120×120×40 voxels was trained to detect and segment the rectum. The 3D U-Net can learn and integrate the relative information between adjacent MRI slices, which can enforce 3D patterns such as rectal wall smoothness and thus compensate for slice-to-slice variability in SNR and rectal boundary fuzziness [0]. Contrast stretching, histogram equalization, and brightness enhancement were also investigated and applied to normalize intra- and inter- image intensity heterogeneity. Data augmentation methods such as elastic deformation, flipping, rotation, and scaling were also applied to reduce the risk of overfitting in model training. The model was trained and tested using a 4-fold cross-validation method with 3:1:2 split for training, validation, and testing. Study results show that the mean intersection over union score (IOUs) is 0.63 for the rectum on the testing dataset. Additionally, visual examination suggests that the displacement between the centroids of the ground truth and inferred volumetric segmentations is less than 3mm. Thus, this study demonstrates that (1) a 3D U-Net model can effectively segment the rectum on low-field MRI scans and (2) applying image processing and data augmentation can boost model performance.

Keywords: Rectum segmentation, Image Registration, 3D U-Net, low-field MRI, prostate biopsy, Deep learning for image segmentation, Computer-assisted image-guided prostate biopsy, Image-to-patient registration for biopsy.

1. INTRODUCTION

Prostate cancer is the second-leading cause of cancer death following in adult men [1]. Approximately one in every eight men is diagnosed with prostate cancer during their lifetime, with a higher risk over age 65 [2]. Early diagnosis via prostate biopsy is key to ensuring patients receive timely and appropriate treatment. The current standard of care is a systematic biopsy (SBx) with transrectal ultrasound (TRUS), which may miss suspicious lesions. Alternatively, targeted biopsy plays an important role in diagnosis and treatment planning [3]. For example, fusion biopsies (FBx) have a pre-procedure diagnostic MRI fused with real-time TRUS, have been used for over a decade, offering urologists an alternative to target precisely specific lesions. However, the variance in registration of pre-procedure diagnostic magnetic resonance imaging (MRI) with the real-time ultrasound can suffer due to the deformation of the prostate gland caused by the TRUS probe. The 3T MRI guidance, where the MRI is performed during the biopsy, does not suffer from this problem but is expensive and not widely available. Low-field (<1T) MRI is a potential solution with the benefits of soft tissue contrast and lower cost, and a similar cancer detection rate compared to in-bore MRI procedures [4].

The rectum is a valuable landmark for registering the pre-procedure, diagnostic, 3T MRI images, where suspected prostate tumors are marked, with the low-field MRI images acquired at the time of biopsy. Adequate visualization of the rectum, as identified on the low-field images and propagated to the 3T MRI images, is essential for fast and accurate image registration. To address and help overcome this clinical difficulty or challenge, we propose and test an automatic rectum segmentation method from the low-field MRI to help reduce the inter-reader variety, automate the tedious manual tasks, and guide the image registration process. If successful, the new image registration method can also reduce the overall image processing time to meet the requirement of the real-time biopsy, as manual registration takes much more time to check and detect the visual similarities between two sets of images. Time is an essential factor as the discomfort of patients grows over time when staying at the operation table in the clinical operation room.

To the best of our knowledge, no similar computer-aided image registration scheme or method to register low-field MRI to the diagnostic MRI has been reported in the literature. The objective of this study is to develop and test an optimal model to automatically segment the rectum depicting on the low-field MR images, which has potential to improve the efficiency and accuracy of subsequent imaging tasks such as image registration in the future.

2. MATERIALS AND METHODS

This IRB-approved and HIPAA-compliant study collected and assembled a retrospective image dataset involving 132 low-field MRI scans acquired from 10 healthy male volunteers (with age ranging from 20 to 60 years). For each scan, the patient was placed in a high lithotomy position, and the pelvis was imaged using a single-sided low-field, MRI system (58-74mT). All images were T2-weighted, but scan length and pulse sequence parameters were varied (ranging from 3 to 22 minutes). The rectum was manually identified and annotated semi-automatically using 3D Slicer. The annotated MRI scans were used as volumetric input data to train the image segmentation models. In brief, the following image processing and segmentation steps are applied in this study.

1. The ground truth annotation of the rectum in MRI was performed using the 3D Slicer software [5], which has been widely used in medical image segmentation and processing [6]. Specifically, the rectum was marked with seeds in the MRI scan, and the region growing was applied to the whole volume to reduce annotation time. A Gaussian smoothing filter was then used to remove the effect of noise on the region-growing step. These steps were scripted in Python and integrated into 3D Slicer to reduce the annotation time. Next, the rectum segmentation was manually adjusted and reviewed to finalize the dataset. All images were 120×120×40 voxels and gray level. A representative image and annotation are shown in Figure 1.

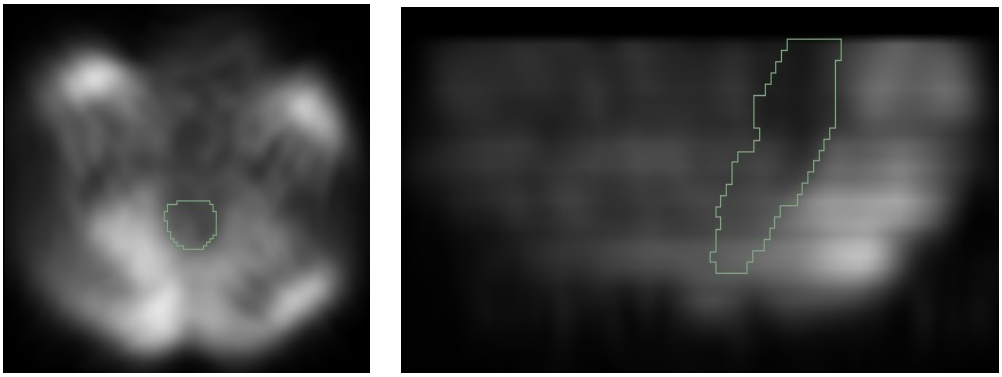

Figure 1: Rectum segmentation annotations in the transverse plane (left) and the sagittal plane (right).

2. Since clinical image quality is affected by multiple factors [7], including patient positioning relative to the MRI hardware, the applied MRI pulse sequences, and possible patient motion during image acquisition, we investigated and compared several image preprocessing methods to compensate for the possible negative effects of these variations in imaging acquisition. These methods include histogram equalization, contrasting stretching, and brightness enhancement [8]. A gamma of 0.5 was chosen for the brightness enhancement. For gamma less than one,

the histogram will shift towards the right, and the output image will be brighter than the input image. A vendor-supplied image denoising algorithm was also used and tested.

3. Due to the limited data set size, data augmentation such as rotation, zooming, flipping, elastic deformation, and shifting was used to mimic the different scanning positions. To be realistic, rotation was limited to less than 10 degrees, and flipping was performed left-right only. For each scan, 15 augmented sets were created for training. There is no augmentation used in the validation or testing set. Different techniques were tested and applied to find an efficient way to generate data [9].

4. Machine learning based computer-aided diagnosis (CAD) tools has great potential in medical imaging applications and have been widely investigated [10-17]. Although many different types of deep learning models have been investigated and developed in previous studies for segmentation tasks, as a proof-of-concept study, we selected one of the most popular segmentation models: U-Net [18]. The model takes the volumetric dataset with the input size of (120, 120, 40) and processes it with alternating 3D convolution and 3D max pooling operations. Each voxel of the output matrix is classified as either rectum or non-rectum, thus outputting a volumetric binary mask. Intersection over union score (IOU) as a metric and 4-fold cross-validation method is used to validate and compare the models with different image normalization methods mentioned in section 2.

3. RESULTS

The ground truth rectum segmentations were visually reviewed and carefully adjusted in consensus by three research scientists with experience in prostate MRIs. This study did not observe disagreement on manual rectum segmentation between reviewers. Thus, the manual segmentation results are accepted in all these annotations.

The computed IOU scores indicate that the developed new image segmentation model performs the best with 2% - 98% percentile contrast stretching with a mean of IOU = 0.63 and a 95% confidence interval (CI) of [0.60, 0.65] as shown and summarized in Table 1.

Table 1: IOUs of rectum segmentation with different image preprocessing applied to the input.

Methods	Mean	95% CI
Contrast Stretching	0.63	[0.6, 0.65]
Brightness Enhancement	0.583	[0.554, 0.612]
Histogram Equalization	0.533	[0.49, 0.576]
No Normalization	0.528	[0.496, 0.56]

Furthermore, we observed that denoised images give a better segmentation than the original images. The 3D model can detect the rectum robustly with different patients and positions. However, some additional islands (false positive voxels) are still on inference segmentation masks. These false rectums are small relative to the true rectum and can be easily removed using post-processing methods such as connected component labeling. One of the rectum segmentations from the inferred model is shown in Figure 2. Another one was rendered as a 3D object in Figure 3.

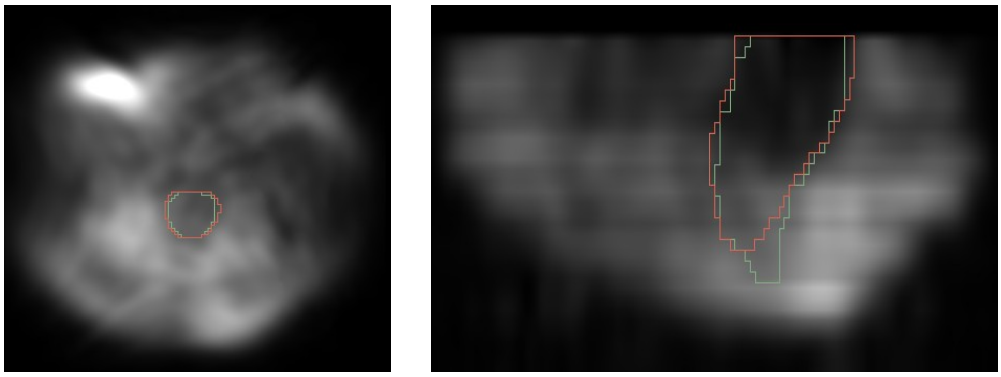

Figure 2: Rectum segmentation in the transverse plane (left) and the sagittal plane (right). The green segmentation is the ground truth, and red segmentation is the output of the model.

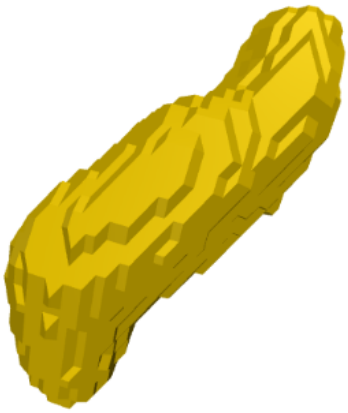

Figure 3: Rendered 3D rectum segmentation from the inferred model. The green segmentation is the ground truth, and the red segmentation is the output of the model.

4. DISCUSSION

In this study, we successfully demonstrate the feasibility and advantages of developing and applying a new deep learning-based 3D image segmentation method or model to segment rectum depicting on the low-field MR images. The contribution of this study to the medical imaging informatics research field includes following.

1) We investigated a new clinical application of applying a deep learning model to segment the rectum on a low-field MRI image, which has the potential to be used as the reference for image registration in MRI-guided prostate biopsy. To our knowledge, no study of a similar topic has been reported in the literature.

2) Although previous segmentation models have been successful on high-resolution and/or high-field MRI images of the prostate and other soft tissue, this study suggests that the 3D U-Net also performs well when presented with the unique challenges of performing well on low-field MRI data of the pelvis. This further suggests it is a robust architecture for similar problems, such as other low-field MRI or motion-sensitive imaging techniques.

3) This study compares the performance of different image processing techniques applied to the original low-field MRI data before they are used to train the 3D U-Net models. We observe that the contrast stretching of the images plays a significant role in determining the segmentation accuracy and robustness of the models.

We also recognize that this preliminary study has several limitations. For example, (1) we have a small number of subjects used in training. However, the images change significantly due to patients positioning and MRI pulse sequence, which generated a large and diverse cohort of images for this segmentation task, (2) the annotations are not performed by radiologists, but with the simple structure of the rectum, our experienced imaging scientists can produce reliable annotations. A board-certified radiologist will review the manual segmentations in the future. Despite these limitations, the study results are encouraging to demonstrate the feasibility of applying a new 3D U-Net model for rectum segmentation on low-field MRI data. If successful, this new method has the potential to benefit the future clinical application of more effective and efficient use of MRI-guided prostate biopsy in future clinical practice. Additional potential applications, such as segmentation of the rectum for dose calculation during MRI-guided brachytherapy or avoidance during MRI-guided focal therapy or biopsy needle insertion, may also benefit from this method.

In summary, based on the foundations established in this preliminary study, we will continue our studies, including but not limited to (1) enforcing the model by changing its architecture to penalize multiple unconnected volumes within a single scan, (2) comparing the performance of 2D and 3D segmentation models on this particular dataset, (3) collect more images to build a more extensive and diverse dataset including additional subjects and collection sites, and (4) develop a new fully automatic registration process for low-field MRI with the 3T diagnostic MRI based on automatic rectum segmentation. Our goal is to improve segmentation accuracy and automate image registration using the segmented rectum and other landmarks in low-field MR images.

ACKNOWLEDMENT

This work is supported in part by the National Institute of General Medical Sciences, National Institutes of Health, under Grant No. P20GM135009.

REFERENCES

[1] Crawford, E.D., “Epidemiology of prostate cancer,” Urology. 62(6), 3-12 (2003).
[2] Siegel, R.L., Miller, K.D., Fuchs, H.E., Jemal, A., “Cancer statistics, 2022,” CA Cancer J Clin. 72(1), 7-33 (2022).
[3] Eklund, M., Jaderling, F., Discacciati, A., et al., “MRI-targeted or standard biopsy in prostate cancer screening,” N Engl J Med. 385, 908-920 (2021).
[4] Satya, P., Adams, J., Venkataraman, S.S., et al., “Office-based, single-sided, low-field MRI-guided prostate biopsy,” Cureus. 14(5), e25021 (2022).
[5] Open source software at www.slicer.org.
[6] Fedorov, A., Beichel, R., Kalpathy-Cramer, J., et al., “3D Slice as an image computing platform for the quantitative imaging network,” Magn Reason Imaging. 30(9), 1323-1341 (2012).
[7] Liu, Y., Kang, J., Li, Z., et al., “Low-dose CT noise reduction based on local total variation and improved wavelet residual CNN,” J Xray Sci Technol. 30(6), 1229-1242 (2022).
[8] Heidari, M., Mirniaharikandehei, S., Khuzani, A.Z., et al., “Improving the performance of CNN to predict the likelihood of COVID-19 using chest X-ray images with preprocessing algorithms,” Int J Med Inform. 144, 104284 (2020).
[9] Kiran Maryada, S., Booker, W.L., Danala, G., et al., “An efficient synthetic data generation algorithm to improve efficacy of deep learning models of medical images,” Research Square. Doi:10.21203/rs.3.rs-2416807/v1 (2022).
[10] Kiran Maryada, S., Booker, W.L., Danala, G., et al., et al., “Applying a novel two-stage deep-learning model to improve accuracy in detecting retinal fundus images,” Proc SPIE. 12033, 120330K (2022).
[11] Heidari, M., Mirniaharikandehei, S., Khuzani, A.Z., et al., “Applying a random projection algorithm to optimize machine learning model for breast lesion classification,” IEEE Trans Biomed Eng. 68(9), 2764–2775 (2021).
[12] Danala, G, Maryada, S.K., Islam, W., et al., “A comparison of computer-aided diagnosis schemes optimized using radiomics and deep transfer learning methods,” Bioengineering. 9(6), 256 (2022).
[13] Naseer, A., Tamoor, M., Azhar, A., “Computer-aided COVID-19 diagnosis and a comparison of deep learners using augmented CXRs,” J Xray Sci Technol. 30(1), 89-109 (2022).

[14] Danala, G., Desai M, Ray B, et al., “Applying quantitative radiographic image markers to predict clinical complications after aneurysmal subarachnoid hemorrhage: A pilot study,” Ann Biomed Eng. 50(4), 413–425 (2022).
[15] Jones, M.A., Islam, W., Faiz, R., et al., “Applying artificial intelligence technology to assist with breast cancer diagnosis and prognosis prediction,” Frontiers in Oncology. 12, 980793 (2022).
[16] Islam, W., Jones, M.A., Faiz, R., et al., “Improving performance of breast lesion classification using a ResNet50 model optimized with a novel attention mechanism,” Tomography. 8(5), 2411-2425 (2022).
[17] Li, T., Liu, Y., Guo, J., Wang, Y., “Prediction of the activity of Crohn’s disease based on CT radiomics combined with machine learning models,” J Xray Sci Technol. 30(6), 1155-1168 (2022).
[18] Ronneberger, O., Fisher, P., Brox, T., “U-Net: Convolutional networks for biomedical image segmentation,” MICCAI. 2015, 234-241 (2015).